Quantum-cascade-laser structures as photodetectors

Daniel Hofstetter,[a] Mattias Beck, and Jérôme Faist
University of Neuchâtel, Institute of Physics, 1 Rue A.-L. Breguet, Neuchâtel, CH 2000 Switzerland

We evaluated two different quantum-cascade-laser structures as photodetectors. The first device was a 5.3 μm two-phonon-resonance structure, and the second one a 9.3 μm bound-to-continuum transition laser. The 5.3 μm structure had a peak responsivity of 120 μA/W at 2200 cm^{-1} and functioned up to 325 K. On the other hand, the 9.3 μm device also worked up to 297 K but had a lower responsivity of 50 μA/W at 1330 cm^{-1}. Since the absorption peak of these devices can be shifted by applying an external bias, we envision interesting applications in free-space optical telecommunications.

Quantum well infrared detectors (QWIPs) for thermal imaging systems have been investigated extensively for several years. Today's state-of-the-art systems consist of arrays with thousands of QWIPs which can detect thermal images at high resolution and with a low background limited infrared performance temperature.[1,2] The detectors used in these systems are optimized for high sensitivity and function usually at cryogenic temperatures. Recently, new applications such as high speed modulators and detectors based on intersubband transitions have been proposed.[3] Because of the short intrinsic carrier lifetimes observed in intersubband transitions, this type of infrared detector should have superior high frequency properties than comparable HgCdTe-based interband photodetectors.[4] Although the responsivity of QWIPs, especially at room temperature, is relatively low, the possibility of having them monolithically integrated with active components, for instance lasers, offers entirely new avenues for telecommunication systems based on intersubband devices. The most important feature of detectors in such systems is their high speed which determines the maximal bandwidth. Although telecommunication experiments using directly modulated quantum-casade (QC) lasers have so far relied on HgCdTe detectors,[5,6] intersubband detectors and intra-cavity modulators seem to be better suited for this task. Accordingly, we present in this article two examples of how QC structures can be used as infrared photodetectors at temperatures up to room temperature.

Growth of the samples for the presented experiments was based on molecular beam epitaxy of lattice matched $In_{0.53}Ga_{0.47}As/In_{0.52}Al_{0.48}As$ layers for S1848 and of strain-compensated $In_{0.6}Ga_{0.4}As/In_{0.44}Al_{0.56}As$ layers for S1869. Both structures were grown on InP substrates; S1848 was a bound-to-continuum transition laser at 9.3 μm, while S1869 was a two-phonon-resonance laser structure with an emission wavelength of 5.3 μm. The two lasers along with the corresponding measurement results are described in detail elsewhere.[7,8] The 9.3 μm bound-to-continuum device was processed into 200×200 μm^2 square mesa structures with a 45° facet for efficient light coupling. For the 5.3 μm device, we chose a 300-μm-long and 40-μm-wide ridge waveguide architecture with a cleaved back facet and a 45° tilted front facet. For testing, we soldered the samples on copper heat sinks and mounted them into a liquid nitrogen flow cryostat. The cryostat was placed in the sample compartment of a Fourier transform infrared spectrometer whose glowbar light source illuminated the sample's 45° facet via an f/1.0 beam condenser. The absolute responsivity values could be determined using a QC laser at 4.6 μm (2200 cm^{-1}). Responsivities of the two detectors were measured at 2200 cm^{-1} and corrected at the respective peak values (2200 cm^{-1} for S1869 and 1330 cm^{-1} for S1848).

As presented in Fig. 1, a comparison between computed and experimentally determined transition energies in S1848 shows reasonable agreement. This is also true under application of a positive bias of up to 6 V. Positive bias means here inversely polarized than when used as laser. Figure 2(a) shows the entire photocurrent spectrum of S1848 measured without bias and for different temperatures between 85 and 210 K. The double peaks are due to transitions from the higher levels (7, 6, 5, and 4) into the two lowest energy levels "1" and "2" which are separated by one optical phonon energy. Indeed, the transition energies in Fig. 1 are separated by about 36 meV. At low temperature, we observed, at

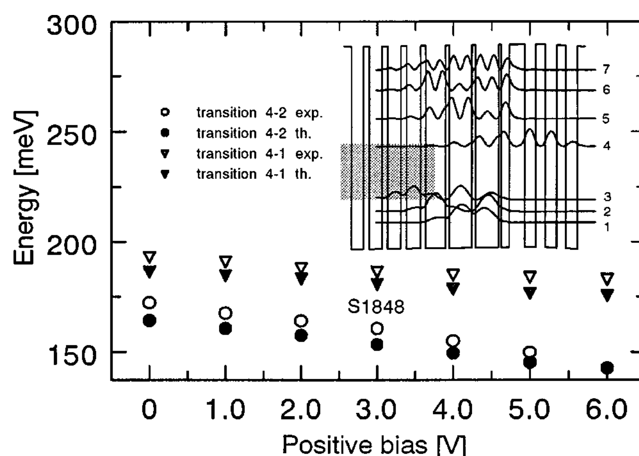

FIG. 1. Measured (empty symbols) and computed (filled symbols) transition energies as a function of applied bias for sample S1848. Shown are the transitions 4-2 (circles) and 4-1 (triangles). The inset shows one period of the conduction band diagram of S1848 at zero bias. The shaded area corresponds to the position of the injector miniband; and the moduli squared of the relevant wave functions are numbered from 1 to 7.

[a]Electronic mail: daniel.hofstetter@unine.ch

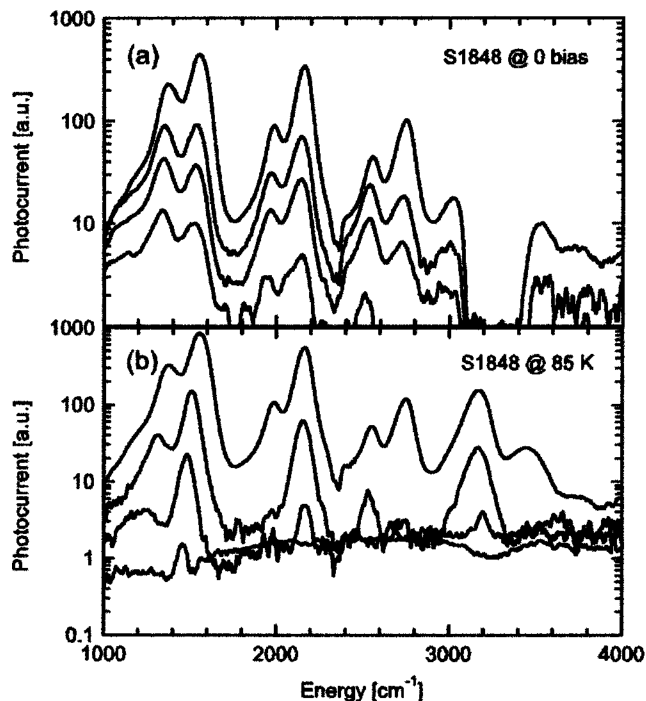

FIG. 2. Photocurrent spectra of sample S1848 as a function of temperature (a) and as a function of positive bias voltage (b). The curves in figure (a) were measured at zero bias and at 85, 135, 160, and 210 K, whereas the curves in figure (b) were at 85 K and with a bias of 0, 2, 4, and 6 V (in both cases going from top to bottom).

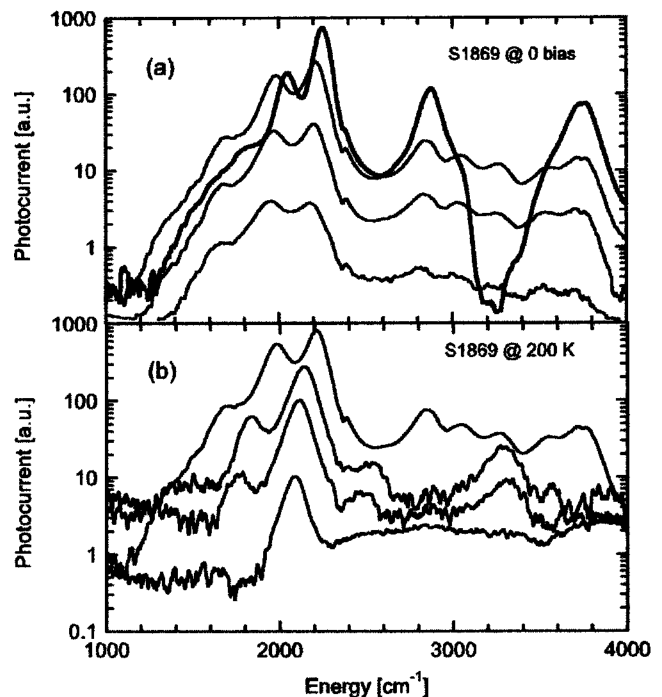

FIG. 3. Photocurrent spectra of sample S1869 as a function of temperature (a) and as a function of positive bias voltage (b). The curves in figure (a) were measured at zero bias and at 85 (bold line), 150 250, and 325 K, whereas the curves in figure (b) were at 200 K and with a bias of 0 (current scale$\times$1.5), 4, 6, and 8 V (in both cases going from top to bottom).

an energy of about 3300 cm^{-1}, a striking absence of signal which can be explained by capturing carriers into impurity levels. As the comparison between Figs. 2(a) and 2(b) shows, this effect is not persistent, especially after having held the sample at low temperatures for a sufficiently long time. In Fig. 2(b), we present a series of photocurrent spectra of S1848 under increasingly positive bias and at 85 K. While the majority of the photocurrent peaks disappear already at +4 V, the two main peaks show at the same time a Stark tuning towards smaller energy and a signal decrease of almost two and a half orders of magnitude. The tallest peak shifted from 1560 to 1450 cm^{-1}; most of the higher energy peaks did not shift because they are due to vertical transitions.

Figure 3(a) is the equivalent measurement to the one in Fig. 2(a), but this time using sample S1869. Due to the deeper quantum wells and therefore a reduced thermionic emission out of the ground state at 5.3 μm, this detector could be used up to room temperature and slightly above (325 K). In addition, its much higher resistance reduced the noise considerably. At 3300 cm^{-1}, impurity features appear as in the former sample. In Fig. 3(b), we show the photocurrent spectra for different positive bias voltages on sample S1869 and at a temperature of 200 K. We observed a similar behavior as with the other sample S1848. By applying +8 V, we were able to decrease the main peak by a factor of 50. At the same time, a Stark shift towards smaller energy, namely from 2200 to 2100 cm^{-1}, was seen.

When measuring the photocurrent under increasingly positive bias at the wavelength of the corresponding laser sample, we saw in both cases a sharp decrease of the detector signal. Again, this was partly due to the net signal reduction at higher bias voltage, but also because of the Stark tuning which shifted the peak away from the laser wavelength. In this configuration, we observed for S1869 (1900 cm^{-1}) a factor of 200 between photocurrent signal without bias and with +8.0 V bias. For the 9.3 μm detector, the effect was less pronounced, but we still got a factor of 25 signal decrease at the lasing wavelength (1100 cm^{-1}) and for 85 K. Under forward bias (negative voltage on the top contact), the signal disappeared completely already at -3 V. While at forward bias, the signal decrease is due to a loss of the electron population into the injector, the signal diminution under positive bias is due to a decrease in photoconductive gain. This hypothesis is supported by the fact that the computed oscillator strengths increase for larger positive biases. At the same time, we observe a decreasing overlap between the upper state of the main QW and the uppermost wave functions of the injector miniband; leading to a net decrease of the escape probability. The external control capability of the absorption peak and the electron population potentially allows the use of such structures as intra-cavity modulators for high-speed modulated QC lasers in free-space telecommunication systems. Because of their small size, such modulators will have a low capacitance, which results in high modulation frequencies.

For the responsivity measurements, we set the external 4.6 μm QC laser at an average output power of 10 mW for the 5.3 μm detector, and an average power of 40 mW for S1848. For S1869, we found a responsivity of 120 μA/W, while in S1848 a value of 50 μA/W was seen. These responsivity values were nearly constant over temperature; however, since the device resistance decreased at higher temperatures, we nevertheless observed a net signal decrease as shown in Figs. 2(a) and 3(a).

As known from the QWIP theory, a good detector should

have negligible interwell tunneling, a constant electron density in the wells, an ideal injection, and finally, a resonance between the upper state of the detector quantum well and the upper band edge of the barrier.[9] In the case of a QC laser structure used as detector, the upper state is also a bound state and therefore cannot be in resonance with the upper band edge. This feature will hamper both escape and capturing probability. As far as the capturing process is concerned, we find that even at zero bias, there is a potential gradient from the injection barrier towards the extraction barrier which also determines the direction of the photocurrent. The dark current points into the same direction under reverse bias, but is opposite under forward bias. Since the injection barrier is very high, the capture probability, p_c, will be essentially 1, even at highly positive bias. The escape probability can be approximately determined using the experimentally known responsivity, R_i, which is related to the photonic gain (and therefore the escape probability) and the quantum efficiency, via $R_i=(e/h\nu)\eta g_{\mathrm{photo}}$. Here, $h\nu$ is the transition energy and e the elementary charge. The quantum efficiency, η, can be calculated with the formula for the intersubband absorption coefficient.[10] This procedure results in roughly $\eta=1\%$. Using this value, we find an escape probability of about $p_e=0.05$. Given an intersubband transition lifetime of 1 ps, we find that the escape time must be on the order of 20 ps; this sounds reasonable given the effective injection barrier height. A comparison of the photoconductive gain, $g_{\mathrm{photo}}=p_e/Np_c$, of a QWIP and a QC laser structure reveals that a QWIP with 35 periods and $p_e=1$ and $p_c=8\times10^{-2}$ would have a photoconductive gain of 0.36, our structures with $p_e=0.05$ and $p_c=1$ would result in $g_{\mathrm{photo}}=1.42\times10^{-3}$; which is a factor of 250 smaller than in the QWIP. Since the responsivity, R_i, depends linearly on the photoconductive gain, we could multiply our values with the above factor 250 in order to have a fairer comparison with the performance of QWIPs.[3]

Clearly, the large capture and small escape probabilities severely reduce the photoconductive gain and thus the responsivity of our detectors. However, in our case the noise gain, $g_n=(1-p_c/2)/Np_c$, becomes small,[11,12] meaning that we might profit from an improved noise behavior. Since our detectors have their best performance at zero bias, there will be no dark current noise. The remaining possible noise contributions are therefore Johnson noise and photon noise. The photon noise, which is given by $I^2_{n,\mathrm{photon}}=4eg_nI_{\mathrm{photon}}\Delta f$, is small for both devices; namely about $I_{n,\mathrm{photon}}=10$ pA. For the Johnson noise, the noise mean square current is given by $I^2_{n,J}=4k_BT\Delta f/R$ with R being the device resistance, k_B the Boltzmann constant, T the temperature, and $\Delta f=30$ kHz the measurement bandwidth. At room temperature ($R=25.4$ kΩ, because of the strain-compensated material with high barriers), we compute for the 5.3 μm device $I_{n,J}=0.14$ nA. For the 9.3 μm detector ($R=66\ \Omega$), the computed $I_{n,J}$ at room temperature is 2.7 nA. The dominant noise source in our detectors must therefore be Johnson noise.

Based on the above results and by defining the noise equivalent power (NEP) via NEP$=I_{n,J}/R_i$, we can give approximate numbers for the detectivity D^* of our detectors. Using $D^*=[(\Delta fA)^{1/2}]$/NEP with A being the device area, we find for S1869 at 2200 cm^{-1} a value of $D^*=1.63\times10^6$ (cm^2 Hz)$^{1/2}$/W, while for S1848 at 1330 cm^{-1}, the corresponding value is 6.41×10^4 (cm^2 Hz)$^{1/2}$/W. According to our considerations about p_c and p_e, QC laser structures used as photodetectors suffer from a factor of about 250 in responsivity. With this factor, D^* would become comparable to literature values of state-of-the-art QWIPs or room temperature HgCdTe detectors.

In conclusion, we have presented two QC laser structures used as infrared detectors. On the basis of the high capture and the low escape probability of the active well, the small responsivity and the low detectivity of these devices are well understood. Due to the fact that a couple of volts is sufficient to shift the absorption peak, we attribute a high application potential to these devices.

The authors gratefully acknowledge device fabrication by Thierry Aellen, helpful discussions with Carlo Sirtori (Thales Research) and H. C. Liu (National Research Council, Ottawa, Canada), and financial support by the Swiss National Science Foundation.

[1] C. G. Bethea, B. F. Levine, V. O. Shen, R. R. Abbott, and S. J. Hsieh, IEEE Trans. Electron Devices **38**, 1118 (1991).
[2] C. G. Bethea, B. F. Levine, M. T. Asom, R. E. Leibenguth, J. W. Stayt, K. G. Glogovsky, R. A. Morgan, J. Blackwell, and W. Parish, IEEE Trans. Electron Devices **40**, 1957 (1993).
[3] H. C. Liu, R. Dudek, A. Shen, E. Dupont, C. Y. Song, Z. R. Wasilewski, and M. Buchanan, Appl. Phys. Lett. **79**, 4237 (2001).
[4] H. C. Liu, J. Li, E. R. Brown, K. A. MacIntosh, K. B. Nichols, and M. J. Manfra, Appl. Phys. Lett. **67**, 1594 (1994).
[5] S. Blaser, D. Hofstetter, M. Beck, and J. Faist, IEEE Electron Device Lett. **37**, 888 (2001).
[6] R. Martini, C. Gmachl, J. Falciglia, F. G. Curti, C. G. Bethea, F. Capasso, E. A. Whittaker, R. Paiella, A. Tredicucci, A. L. Hutchinson, D. L. Sivco, and A. Y. Cho, IEEE Electron Device Lett. **37**, 102 (2001).
[7] D. Hofstetter, M. Beck, T. Aellen, and J. Faist, Appl. Phys. Lett. **78**, 396 (2001).
[8] J. Faist, M. Beck, T. Aellen, and E. Gini, Appl. Phys. Lett. **78**, 147 (2001).
[9] H. C. Liu, in *Semiconductors and Semimetals*, edited by H. C. Liu and F. Capasso (Academic, San Diego, 2000), Vol. 62, Chap. 3, p. 126.
[10] M. Helm, in *Semiconductors and Semimetals*, edited by H. C. Liu and F. Capasso (Academic, San Diego, 2000), Vol. 62, Chap. 1, p. 5.
[11] W. A. Beck, Appl. Phys. Lett. **63**, 3589 (1993).
[12] C. Schönbein, H. Schneider, R. Rehm, and R. Walther, Appl. Phys. Lett. **73**, 1251 (1998).